Electronic Supplementary Material (ESI) for Journal of Materials Chemistry A.

Supporting Information

Highly Efficient Layer-by-Layer Large-Scale Manufacturing Polymer Solar Cells with Minimized Device-to-Device Variations by Employing Benzothiadiazole-Based Solid Additives

Jiyeon Oh,[†a] Sungwoo Jung,[†a] So-Huei Kang,[a,b] Geunhyung Park,[a] Mingyu Jeong,[a] Seoyoung Kim,[a] Seunglok Lee,[a] Wonjun Kim,[a] Byongkyu Lee,[a] Sang Myeon Lee,[a,c] and Changduk Yang*[a]

[a] School of Energy and Chemical Engineering, Perovtronics Research Center, Low Dimensional Carbon Materials Center, Ulsan National Institute of Science and Technology (UNIST), 50 UNIST-gil, Ulju-gun, Ulsan 44919, South Korea.

[b] Department of Chemistry, McGill University, 801 Sherbrooke St West, Montreal, QC H3 A 0b8, Canada

[c] 4th R&D Institute-6th Directorate, Agency for Defense Development, Yuseong-Gu, Daejeon 34186, Korea

[†]J. O and S. J contributed equally to this work

[*] E-mail: yang@unist.ac.kr

Experimental Section

Materials and instrument: All the chemicals and reagents were purchased from Sigma-Aldrich, Alfa Aesar chemical company, and Tokyo Chemical Industry Co., Ltd. without any further purification. All solvents were ACS grade unless otherwise noted. BT (2,1,3-Benzothiadiazole) was purchased from Combi-Blocks. FBT and 2FBT were synthesized according to previously reported literature.[23] PM6, *L*-PM6, *H*-PM6, and *H*-PTQ10 were synthesized according to the previously reported methods.[24] PTQ10 was purchased from Brilliant Matters (M_n: 19.1 kDa, M_w: 40.9 kDa, PDI: 2.14). Y6 and BTP-eC9 were purchased from eflexPV. The molecular weights of the PM6 and PTQ10 were characterized with high-temperature gel permeation chromatography (HR-GPC) at 100 °C using polystyrene as the standard in 1,2,4-trichlorobenzene (HPLC grade). The FT-IR absorption spectra were measured on a Varian 670 infrared spectrometer with wavenumber ranging from 1000 to 4000 cm^{-1}. The solutions for FT-IR absorption spectra were prepared by PM6 films with BT solid additives of optimized weight ratio in chloroform with same concentration of 8mg mL^{-1}.

Synthesis of PM6: Diorganobromide (500 mg, 0.532 mmol) and diorganostanne (407.6 mg, 0.532 mmol) compounds were dissolved in toluene (22.5 ml) in a two-neck round flask and then purged with argon for 30 min. A solution of $Pd(PPh_3)_4$ (24.6 mg, 0.021 mmol) in anhydrous toluene (2.5 ml) was added to the mixture in one portion in an argon state. Then the mixture was heated at 120 °C in a pre-heated oil bath for 12 h. The resulting polymers were precipitated in methanol, followed by Soxhlet extraction in sequence of methanol, acetone, and n-hexane. Finally, the chloroform fraction was extracted and reprecipitated in methanol to get the target product (M_n: 41.3 kDa, M_w: 109.7 kDa, PDI: 2.66).

Synthesis of L-PM6: According to the procedure described above, the mixture was heated at 120 °C in a pre-heated oil bath for 9 h to synthesize *L*-PM6 (M_n: 30.4 kDa, M_w: 106.9 kDa, PDI: 3.51).

Synthesis of H-PM6: According to the procedure described above, the mixture was heated at 120 °C in a pre-heated oil bath for 36 h to synthesize *H*-PM6 (M_n: 49.3 kDa, M_w: 144.7 kDa, PDI: 2.93).

Synthesis of H-PTQ10: 2,5-bis(trimethylstannyl)thiophene (82.0 mg, 0.2 mmol) and 5,8-dibromo-6,7-difluoro-2-((2-hexyldecyl)oxy)quinoxaline (112.9 mg, 0.2 mmol) were dissolved in anhydrous toluene (6 mL) in a long Schlenk flask, and purged with argon for 20 min. Then,

of tetrakis(triphenylphosphine)palladium(0) (6.9 mg, 0.006 mmol) was added and purged again with argon for 20 min. The reaction mixture was stirred at 110 °C for 36 h. After cooling down, the crude mixture was poured into methanol, then transferred to thimble filter. Sequential Soxhlet extraction with methanol, acetone, and hexane was performed to remove low molecular weight fractions. The residue was extracted with chloroform, concentrated, and precipitated to methanol. The purified polymer was collected by filtration and dried in high vacuum oven (M_n: 46.7 kDa, M_w: 111.8 kDa, PDI: 2.39).

Device fabrication and characterization: The patterned ITO-coated glass substrates were rinsed using detergent, acetone and isopropanol and were subsequently dried overnight in an oven. The substrate size of 1.5 cm x 1.5 cm was employed for the devices with area of 0.048 and 0.92 cm^2, while the substrate (2.5 cm x 2.5 cm) was used in the device with 2.50 cm^2. All the LBL PSCs were fabricated using the same conditions and procedures. PM6/Y6 based LBL device was fabricated with a configuration of ITO/PEDOT:PSS/PM6/Y6/PDINO/Al. PEDOT:PSS (Bayer Baytron 4083) was spin-coated at 4000 rpm onto an ITO substrate, followed by annealing at 140 °C for 10 min in air. As for the LBL PSCs, PM6 solution was prepared in chloroform at 8 mg mL^{-1} with 10 to 40% (w/w) BT solid additives of the PM6 concentration. Y6 solution was prepared in chloroform at 9 mg mL^{-1} with 0.5% CN of the solvent volume. The PM6 solution was spin-coated on the PEDOT:PSS film at 2200 rpm for 60 s, and then annealed at 100 °C for 5 min. Y6 is deposited on the PM6 film at 2300 rpm for 60 s with annealing at 100 °C for 5 min. In case of PTQ10/Y6 based device, PTQ10 and Y6 were prepared at 7 mg mL^{-1} and 9 mg mL^{-1} respectively. For PM6/BTP-eC9 based device, the device structure of ITO/PEDOT:PSS/PM6/BTP-eC9/PFN-Br/Ag. PM6 was prepared at 7 mg $mL^{-}$and BTP-eC9 with concentration of 9 mg mL^{-1}. The donor polymer film with FBT additive was treated with thermal annealing at 100 °C for 5 min, and then the acceptor film is processed with annealing at 100 °C for 5 min. Then, a methanol solution of PDINO (1.0 mg mL^{-1}) or PFN-Br (0.5 mg mL^{-1}) was spin-coated onto the active layer with a spin rate of 3000 rpm for 30 s. Finally, a 100 nm Al or Ag cathode was thermally evaporated on top of the substrates under vacuum (<3.0 x 10^{-6} Pa).

The *J–V* characteristics were measured on a Keithley 2400 source under the illumination of an AM 1.5G solar simulator with an intensity of 100 mW cm^{-2}. EQE measurements were conducted using Model QE-R3011 (Enli Technology) in ambient air. The hole and electron

mobilities were measured via using the SCLC method. Device structures are ITO/PEDOT:PSS/Donor/Acceptor/Au for hole-only devices and ITO/ZnO/Donor/Acceptor/Al for electron-only devices, respectively. The SCLC mobilities were calculated using the Mott–Gurney equation, $J_{SCLC} = (9/8)\varepsilon_0\varepsilon_r\mu((V^2)/(L^3))$, where ε_r is the relative dielectric constant of the organic semiconductor, ε_0 is the permittivity of empty space, μ is the mobility of zero-field, L is the thickness of the active layer, and *V* is applied voltage across the device. XPS was measured using K-alpha.

Morphology characterization: AFM images of thin films were obtained using multimode V microscope (Veeco, USA) with a nanscope controller using Si tips (Bruker). TEM analysis was performed using a JEOL USA JEM-2100F (Cs corrector) transmission electron microscope. GIWAXS was carried out at the PLS-II 6D U-SAXS and 9A beamline of the Pohang Accelerator Laboratory in Korea. The scattering signal was recorded using a 2-D CCD detector (Rayonix SX165). The X-ray light had an energy of 11.24 KeV. The incidence angle of X-rays was adjusted to 0.09-0.12 to maximize the signal to background ratio.

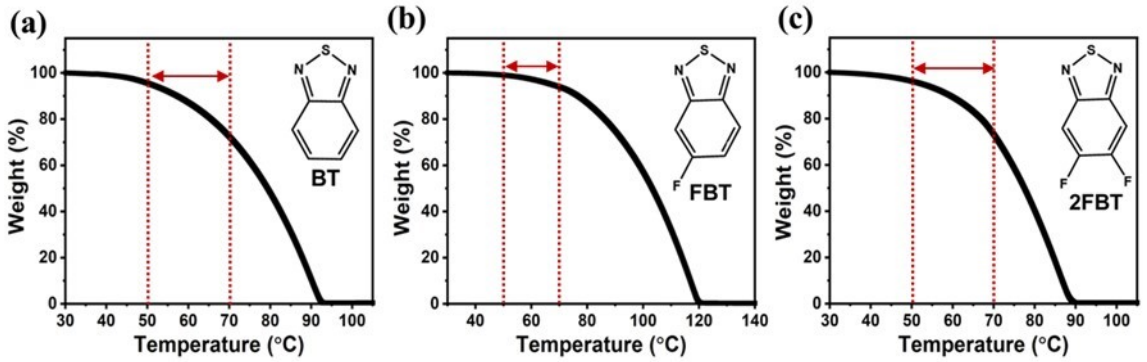

Fig. S1 TGA plots of a) BT, b) FBT and c) 2FBT material at a scan rate of 10 °C min^{-1}.

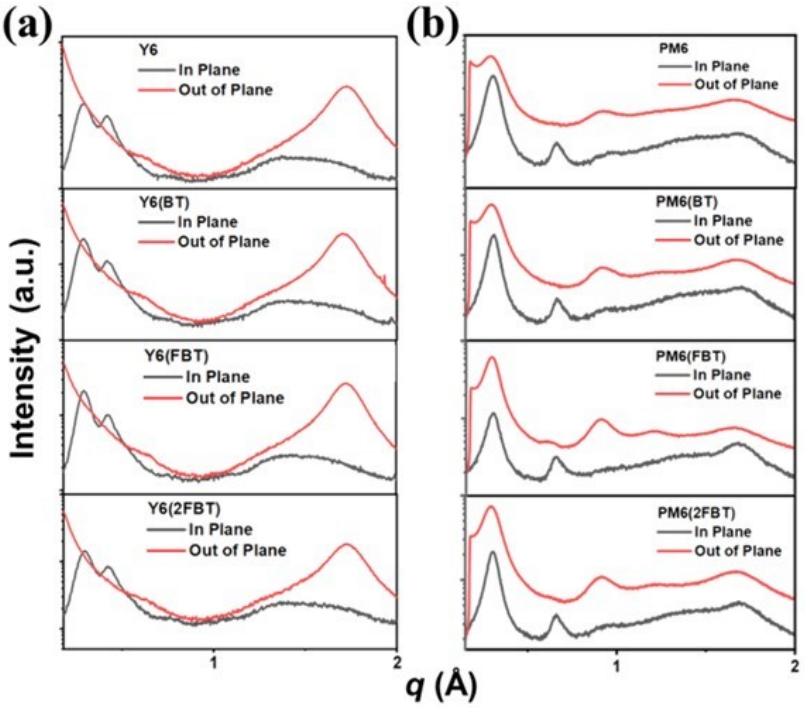

Fig. S2 line cut profiles of the a) Y6 films and b) PM6 without and with BT solid additives.

Table S1 Lattice parameters for Y6 neat films without and with BT solid additives.

System	Out-of-Plane				In-Plane			
	***π*-*π* stacking (010)**				**Lamellar packing (100)**			
	***q* (Å^{-1})**	***d*-spacing (Å)**	**FWHM (Å^{-1})**	**Coherence length (Å)**	***q* (Å^{-1})**	***d*-spacing (Å)**	**FWHM (Å^{-1})**	**Coherence length (Å)**
Y6	1.721	3.650	0.191	29.873	0.297	21.160	0.084	67.429
Y6(BT)	1.710	3.672	0.197	28.955	0.291	21.611	0.082	68.982
Y6(FBT)	1.725	3.643	0.205	27.906	0.293	21.471	0.074	68.731
Y6(2FBT)	1.727	3.638	0.207	27.638	0.295	21.303	0.083	68.607

Table S2 Lattice parameters for PM6 neat films without and with BT solid additives.

System	Out-of-Plane							
	***π*-*π* stacking (010)**				**Lamellar packing (*h*00)**			
	***q* (Å^{-1})**	***d*-spacing (Å)**	**FWHM (Å^{-1})**	**Coherence length (Å)**	***q* (Å^{-1})**	***d*-spacing (Å)**	**FWHM (Å^{-1})**	**Coherence length (Å)**
PM6	1.636	3.840	0.370	15.427	0.918	6.842	0.157	36.195
PM6(BT)	1.662	3.775	0.212	26.979	0.919	6.840	0.144	39.295
PM6(FBT)	1.650	3.809	0.276	20.672	0.912	6.890	0.118	47.966
PM6(2FBT)	1.655	3.797	0.199	28.684	0.911	6.900	0.138	41.223

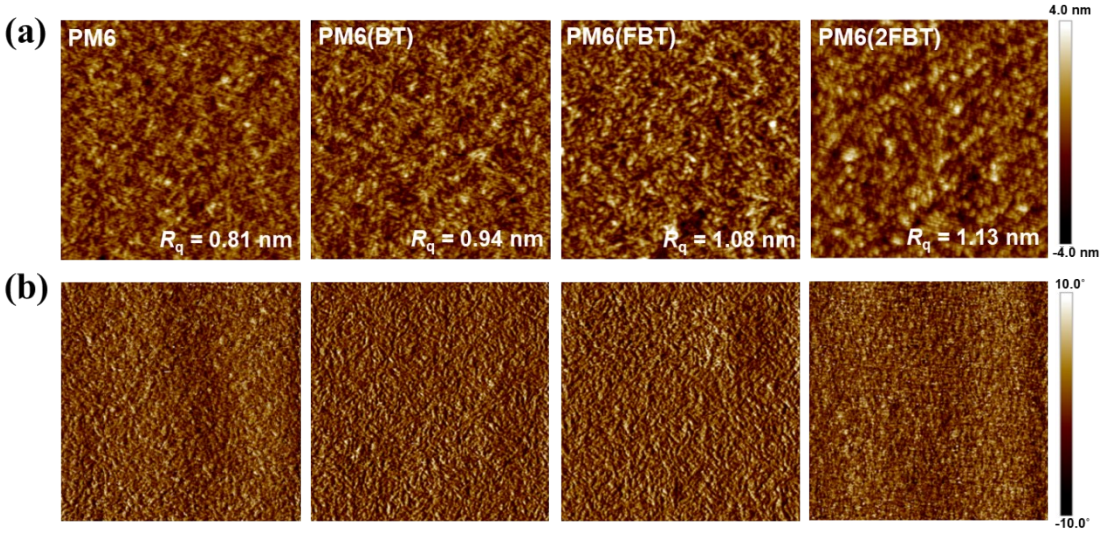

Fig. S3 a) Height and b) phase AFM images (scan size 2 x 2 μm) of PM6 neat films without and with BT solid additives.

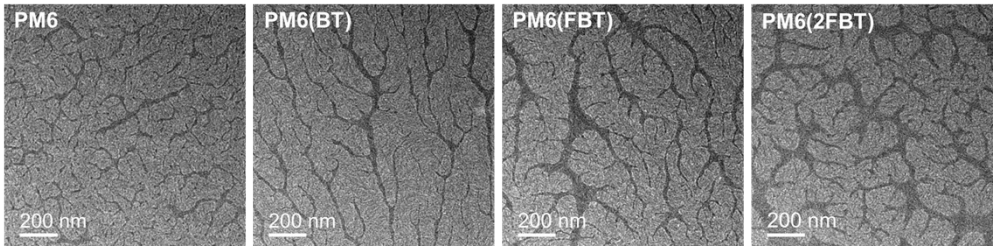

Fig. S4 TEM images of PM6 neat films without and with BT solid additives (magnification of 15.5k).

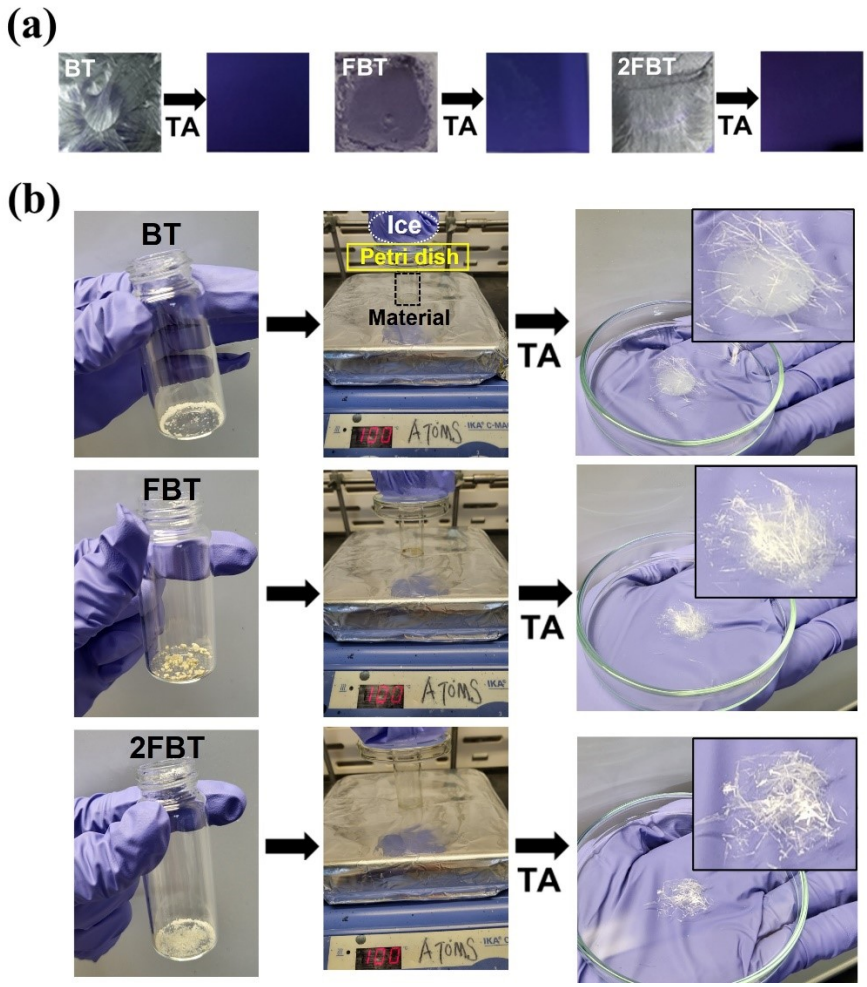

Fig. S5 Photographs of BT solid additives (a) film on the Si substrate and (b) bulk in the vial followed by thermal annealing at 100 °C for 5 min.

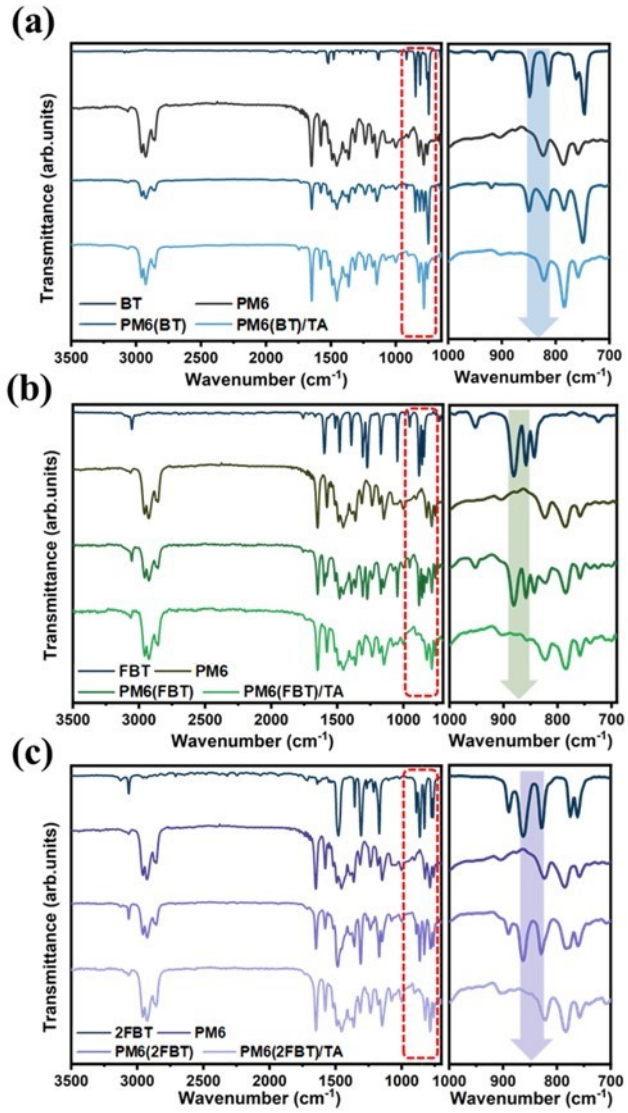

Fig. S6 FT-IR spectra of PM6 films with a) BT, b) FBT, and c) 2FBT under TA at 80 °C for 5 min.

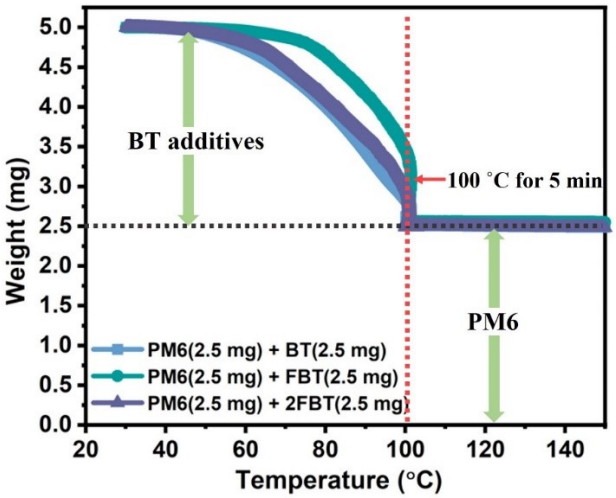

Fig. S7 TGA plot of PM6:BT-solid additives (weight ratio of 1:1) at a scan rate of 10.0 ℃ min^{-1} and in the heating process, the temperature was held for 5 min at 100 ℃.

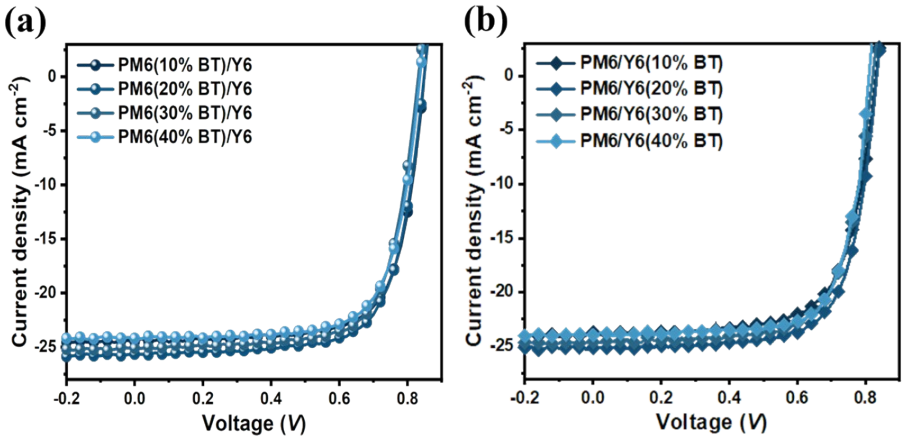

Fig. S8 *J-V* curves of the PM6/Y6 LBL system with a different weight ratio of BT additive on a) donor and b) acceptor layer.

Table S3 Summary of device parameters of PM6/Y6 devices with different weight ratios of BT additive on donor or acceptor layer under illumination of AM 1.5G (100 mW cm^{-2}).

System	V_{OC} [a)] [V]	J_{SC} [a)] [mA cm^{-2}]	FF [a)] [%]	PCE [a)] [%]
PM6(10% BT)/Y6	0.849 (0.843)	24.58 (24.20)	71.52 (71.23)	14.93 (14.51)
PM6(20% BT)/Y6	0.849 (0.842)	25.70 (25.17)	71.02 (70.45)	15.49 (15.21)
PM6(30% BT)/Y6	0.843 (0.840)	25.05 (24.88)	70.87 (70.68)	14.97 (14.76)
PM6(40% BT)/Y6	0.840 (0.832)	24.17 (23.85)	70.60 (70.35)	14.33 (13.93)
PM6/Y6(10% BT)	0.836 (0.836)	24.48 (24.39)	70.24 (70.03)	14.37 (14.28)
PM6/Y6(20% BT)	0.835 (0.833)	25.13 (24.87)	70.78 (70.61)	14.85 (14.63)
PM6/Y6(30% BT)	0.832 (0.831)	24.60 (24.43)	70.55 (70.37)	14.44 (14.29)
PM6/Y6(40% BT)	0.822 (0.819)	24.06 (23.65)	70.26 (69.57)	13.89 (13.38)

[a)] the statistical values in parentheses are obtained from 16 cells.

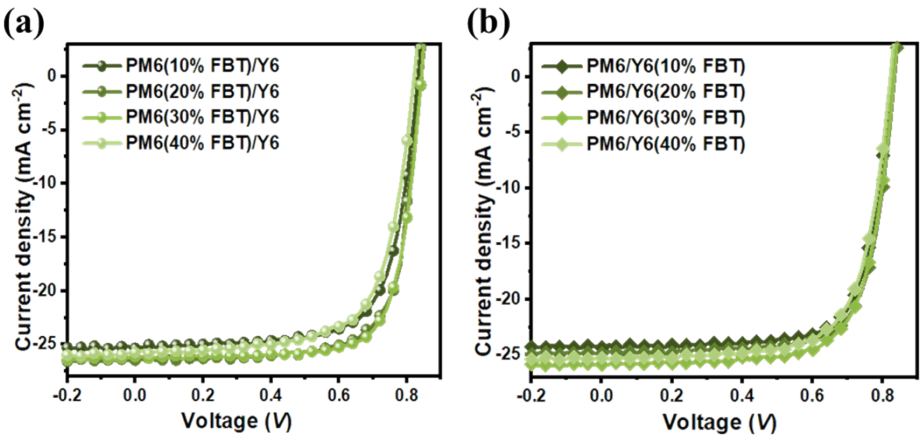

Fig. S9 *J-V* curves of the PM6/Y6 LBL system with a different weight ratio of FBT additive on a) donor and b) acceptor layer.

Table S4 Summary of device parameters of PM6/Y6 devices with different weight ratios of FBT additive on donor or acceptor layer under illumination of AM 1.5G (100 mW cm^{-2}).

System	V_{OC} [a)] [V]	J_{SC} [a)] [mA cm^{-2}]	FF [a)] [%]	PCE [a)] [%]
PM6(10% FBT)/Y6	0.845 (0.840)	25.19 (24.93)	74.90 (73.67)	15.94 (15.43)
PM6(20% FBT)/Y6	0.843 (0.841)	25.73 (25.36)	75.72 (75.48)	16.42 (16.09)
PM6(30% FBT)/Y6	0.842 (0.840)	26.14 (25.83)	75.31 (75.19)	16.63 (16.31)
PM6(40% FBT)/Y6	0.838 (0.835)	25.44 (25.20)	73.22 (72.81)	15.61 (15.32)
PM6/Y6(10% FBT)	0.833 (0.832)	24.74 (24.35)	71.27 (71.06)	14.69 (14.39)
PM6/Y6(20% FBT)	0.833 (0.833)	25.02 (24.88)	71.52 (71.32)	14.91 (14.78)
PM6/Y6(30% FBT)	0.831 (0.828)	25.48 (25.15)	71.68 (71.27)	15.40 (15.03)
PM6/Y6(40% FBT)	0.825 (0.825)	25.28 (25.08)	70.84 (70.55)	14.77 (14.60)

[a)] the statistical values in parentheses are obtained from 16 cells.

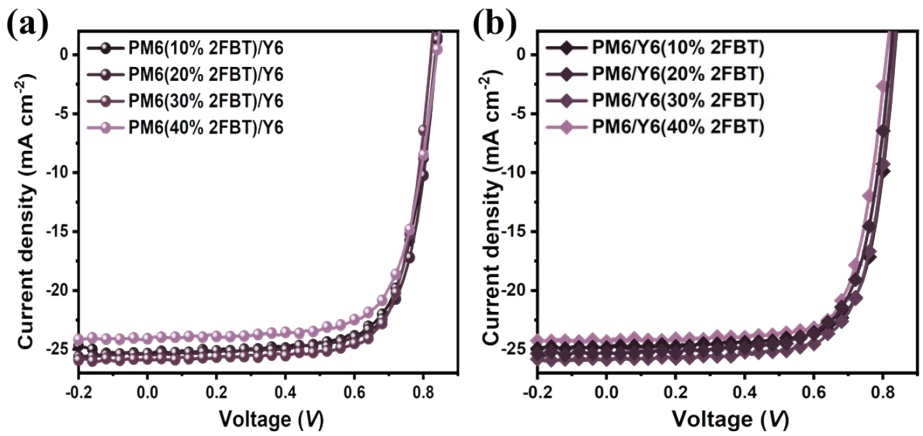

Fig. S10 *J-V* curves of the PM6/Y6 LBL system with a different weight ratio of 2FBT additive on a) donor and b) acceptor layer.

Table S5 Summary of device parameters of PM6/Y6 devices with different weight ratios of 2FBT additive on donor or acceptor layer under illumination of AM 1.5G (100 mW cm^{-2}).

System	V_{OC} [a)] [V]	J_{SC} [a)] [mA cm^{-2}]	FF [a)] [%]	PCE [a)] [%]
PM6(10% 2FBT)/Y6	0.842 (0.840)	25.43 (24.81)	70.02 (69.83)	14.99 (14.54)
PM6(20% 2FBT)/Y6	0.840 (0.842)	25.71 (25.41)	71.32 (70.90)	15.40 (15.17)
PM6(30% 2FBT)/Y6	0.839 (0.834)	25.83 (25.41)	72.88 (72.30)	15.79 (15.32)
PM6(40% 2FBT)/Y6	0.835 (0.833)	24.52 (23.95)	71.47 (71.14)	14.63 (14.20)
PM6/Y6(10% 2FBT)	0.835 (0.835)	24.67 (24.37)	70.03 (69.88)	14.43 (14.22)
PM6/Y6(20% 2FBT)	0.834 (0.833)	24.93 (24.81)	70.42 (70.27)	14.64 (14.52)
PM6/Y6(30% 2FBT)	0.830 (0.830)	25.31 (25.18)	70.98 (70.75)	14.91 (14.78)
PM6/Y6(40% 2FBT)	0.828 (0.826)	24.22 (24.00)	70.56 (70.36)	14.15 (13.95)

[a)] the statistical values in parentheses are obtained from 16 cells.

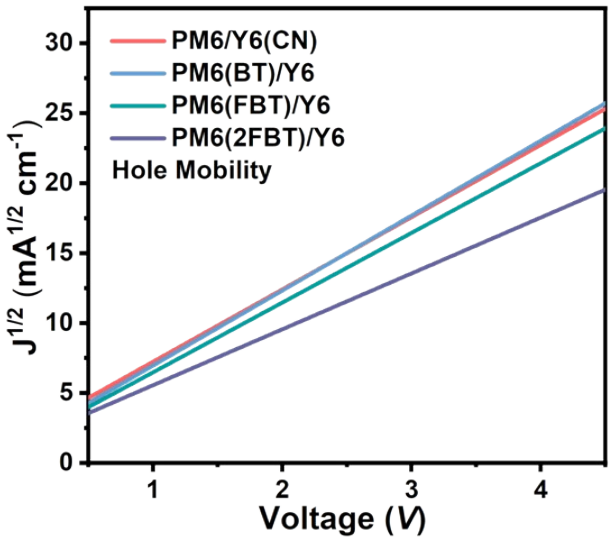

Fig. S11 SCLC plots of hole only devices with PM6/Y6 LBL system with optimized additives.

Table S6 Hole mobility parameters of the PM6/Y6 devices with optimized additives**.**

System	μ_h [$cm^2V^{-1}s^{-1}$]
PM6/Y6(CN)	4.92×10^{-4}
PM6(BT)/Y6	5.12×10^{-4}
PM6(FBT)/Y6	5.67×10^{-4}
PM6(2FBT)/Y6	5.49×10^{-4}

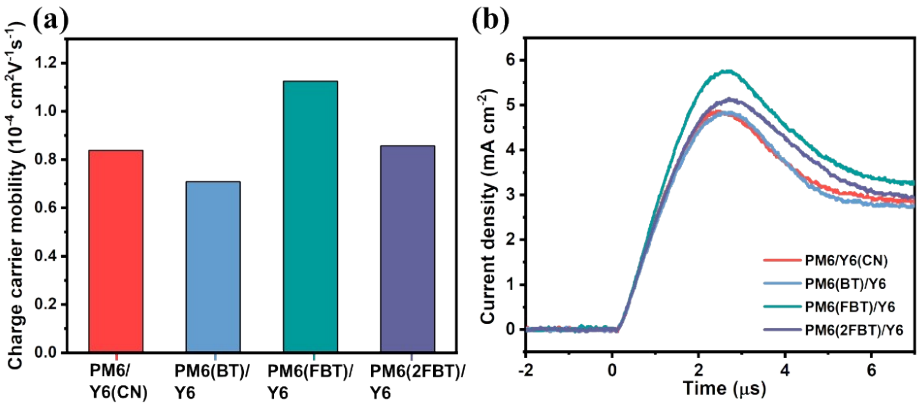

Fig. S12 a) Charge carrier mobility of LBL-based devices calculated from photo-CELIV. b)Photo-CELIV measurement on the optimized devices.

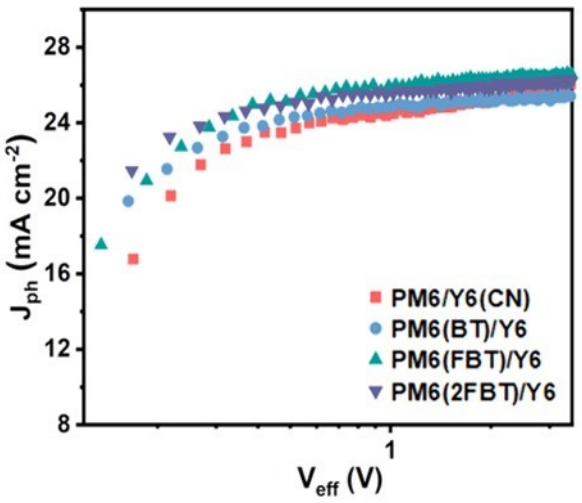

Fig. S13 J_{ph} versus V_{eff} plots of the PM6/Y6 PSCs with optimized additives.

Table S7 Exciton dissociation probabilities and charge extraction probabilities of the devices.

System	Exciton dissociation probability (%)	Charge extraction probability (%)
PM6/Y6(CN)	97.71	76.21
PM6(BT)/Y6	97.42	75.06
PM6(FBT)/Y6	99.13	78.88
PM6(2FBT)/Y6	98.81	77.35

Table S8 Lattice parameters in out-of-plane and in-plane direction for LBL active layer films with optimized additives.

System	Out-of-Plane				In-Plane			
	***π*-*π* stacking (010)**				**Lamellar packing (100)**			
	***q* (Å^{-1})**	***d*-spacing (Å)**	**FWHM (Å^{-1})**	**Coherence length (Å)**	***q* (Å^{-1})**	***d*-spacing (Å)**	**FWHM (Å^{-1})**	**Coherence length (Å)**
PM6/Y6(CN)	1.721	3.650	0.219	26.168	0.309	20.334	0.079	71.605
PM6(BT)/Y6	1.708	3.678	0.223	25.614	0.303	20.712	0.078	72.522
PM6(FBT)/Y6	1.709	3.672	0.215	26.646	0.305	20.579	0.074	76.308
PM6(2FBT)/Y6	1.713	3.667	0.211	27.090	0.304	20.654	0.074	76.754

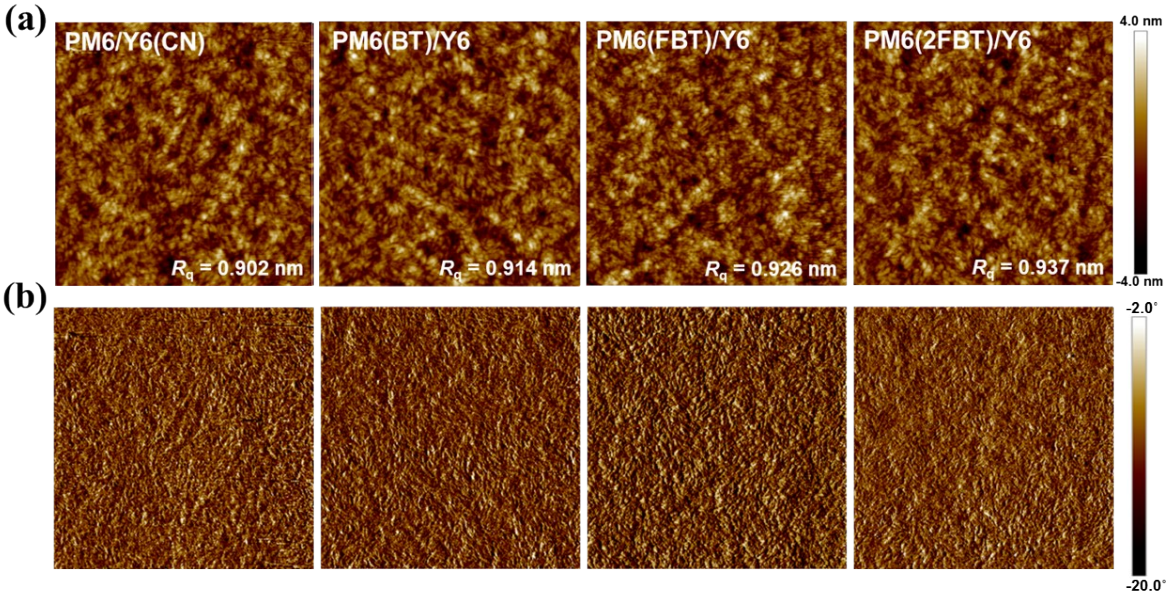

Fig. S14 a) Height and b) phase AFM images (scan size 2 x 2 μm) of PM6/Y6 LBL system with optimized additives.

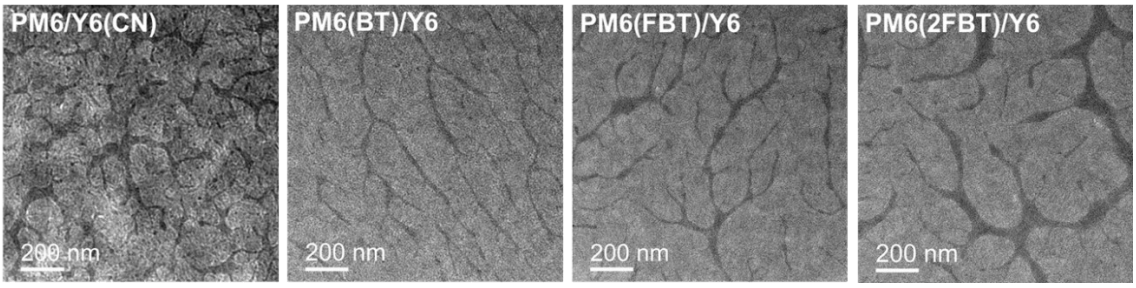

Fig. S15 TEM images of PM6/Y6 LBL system with optimized additives (magnification of 15.5k).

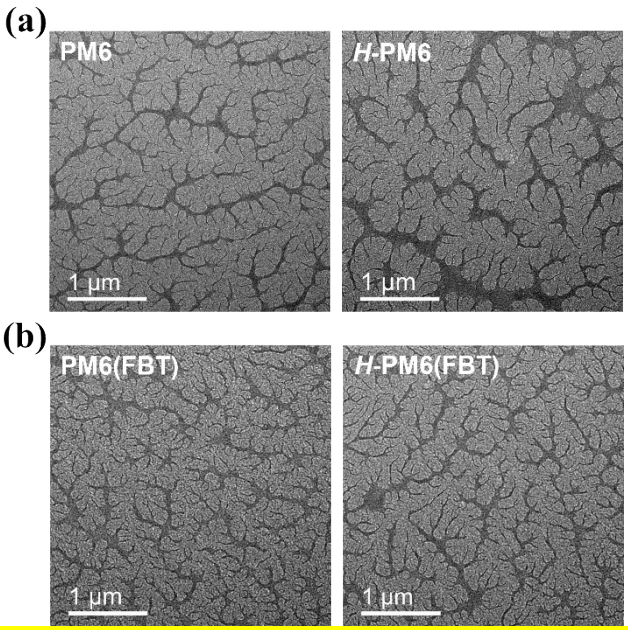

Fig. S16 TEM images of PM6 neat films with different molecular weights depending on the a) without and b) with FBT solid additive (magnification of 5.6k).

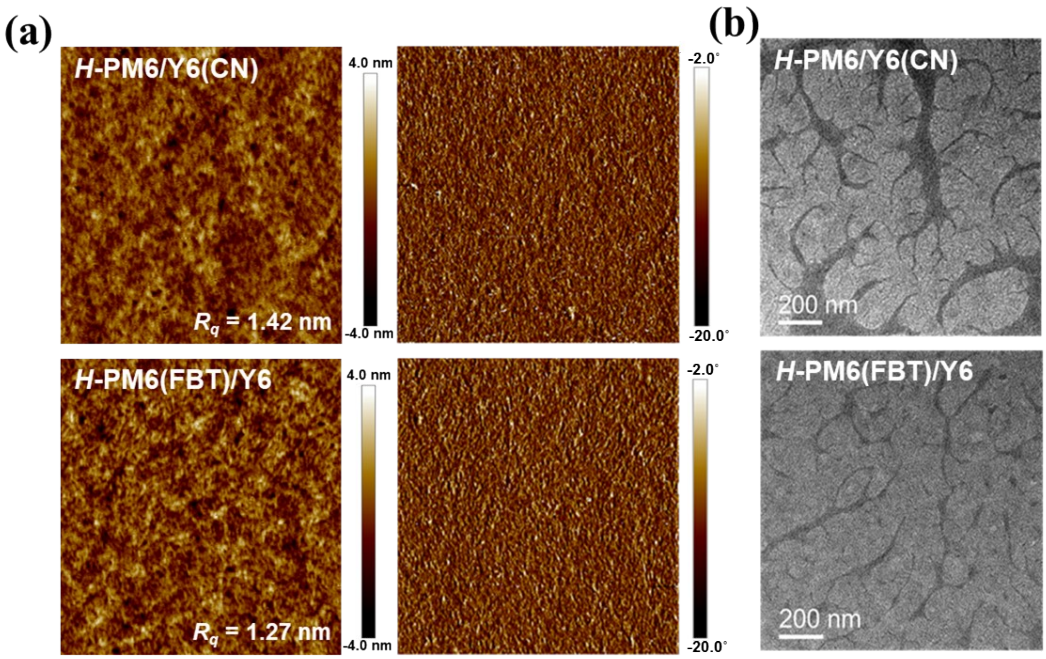

Fig. S17 a) AFM (scan size 2 x 2 μm) and b) TEM images (magnification of 15.5k) of *H*-PM6/Y6 LBL system with optimized additives.

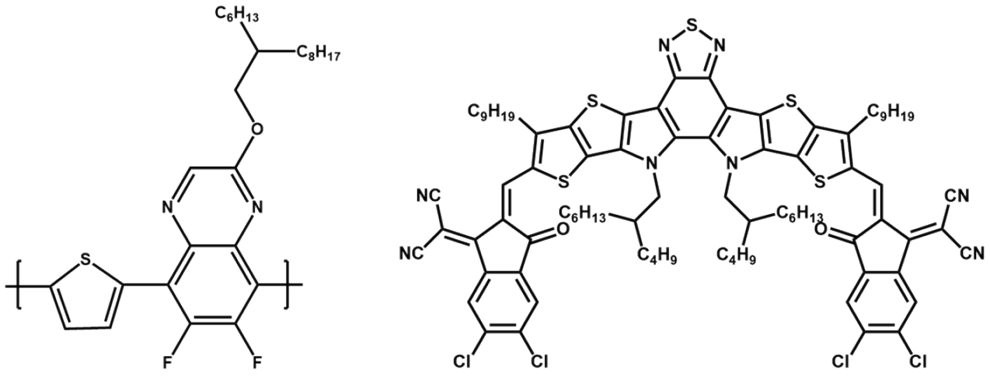

Fig. S18 Chemical structures of PTQ10 and BTP-eC9.

Table S9 Summary of recently reported LBL PSCs.

Year	Active layer	Processing Solvent	V_{OC} [V]	J_{SC} [mA cm^{-2}]	FF [%]	PCE [%]	Reference
2019	PTQ10/IDIC	CF/CF	0.943	18.75	69.66	12.32	1
2020	PTQ10/Y6	CF/CF	0.849	24.49	72.63	15.10	2
2020	PM6/Y6-2Cl	CF/CF	0.849	25.88	72.30	15.89	2
2020	PM6/Y6-C2	CF/CF	0.834	25.82	73.99	15.93	2
2020	PM6/Y6	CF/CF	0.840	25.22	72.49	16.35	2
2020	PT2/Y6	CB/CF	0.83	26.7	74.4	16.5	3
2021	PM6/Y6	CB/CF	0.800	24.5	73.5	14.42	4
2021	PM6/N3:PC71BM	CF/CF	0.841	26.49	78.2	17.42	5
2021	PM6/BTP-eC9	*o*-xylene/*o*-xylene	0.840	26.65	78.1	17.48	6
2021	PM6/BTP-eC9	CF/CF	0.839	26.91	77.7	17.54	6
2021	PM6/BO-4Cl:BTP-S2	CF/CF	0.861	27.14	78.04	18.16	7
2022	PM6/Y6	CF/CF	0.861	25.76	73.67	16.35	8
2022	PM6/Y6:TIT-2Cl	CF/CF	0.876	26.63	77.93	18.18	8

Table S10 Summary of recently reported PM6-based PSCs treated with volatile solid additives.

Year	System	Active layer	Additive	V_{OC} [V]	J_{SC} [mA cm^{-2}]	FF [%]	PCE [%]	Reference
2020	BHJ	PM6:Y6	Ferrocene	0.838	26.71	76.0	17.40	9
2020	BHJ	PBDB-T-2F:BTP-4F	INB-5F	0.81	27.7	74.3	16.4	10
2020	BHJ	PM6:TPT10	BDT-1	0.899	24.80	73.00	16.26	11
2021	BHJ	PBDB-TF:BO4Cl	DTBF	0.846	26.2	77.0	17.1	12
2021	BHJ	PM6:Y6	Anthracene	0.844	25.91	77.8	17.02	13
2021	BHJ	PM6:Y6	A3	0.82	26.50	76.05	16.5	14
2021	LBL	PM6/Y6	DDO	0.85	25.51	77.45	16.93	15
2021	LBL	PBDB-TF/Y6	DTBF	0.823	26.0	76.6	16.4	16
2022	**LBL**	**PM6/BTP-eC9**	**FBT**	**0.835**	**26.68**	**79.52**	**17.71**	**Our Work**

Table S11 PCE variations according to molecular weights of donor polymer on different systems.

System	ΔPCE [a)]
PTQ10/Y6(DIO)	1.32
H-PTQ10/Y6(DIO)	
PTQ10(FBT)/Y6	1.14
H-PTQ10(FBT)/Y6	
PM6/BTP-eC9(DIO)	1.86
H-PM6/BTP-eC9(DIO)	
PM6(FBT)/BTP-eC9	1.52
H-PM6(FBT)/BTP-EC9	

[a)] the values follow this equation ($PCE_{donor/acceptor}$-$PCE_{H\text{-}donor/acceptor}$)

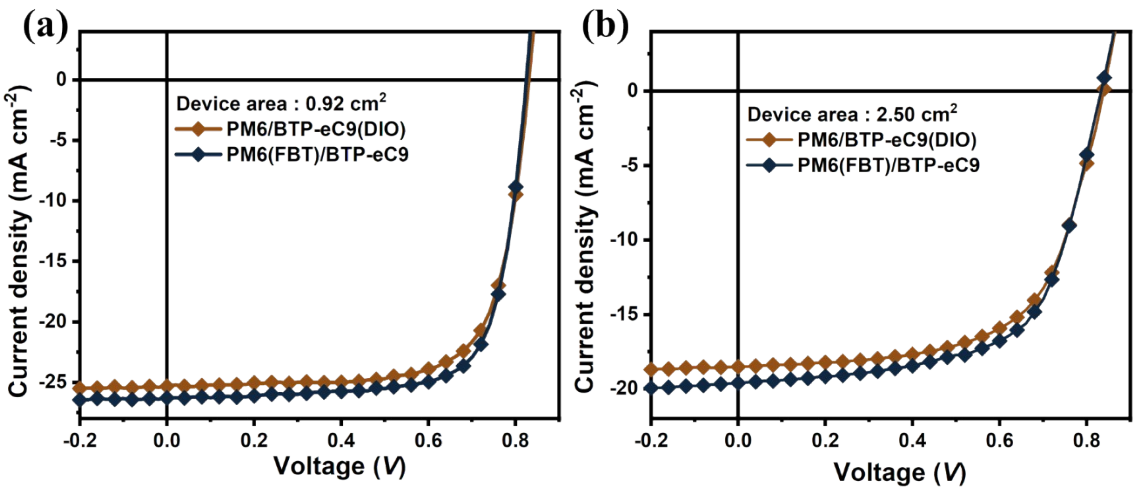

Fig. S19 *J-V* curves of the PM6/BTP-eC9 LBL devices at (a) 0.92 cm^2 and (b) 2.50 cm^2.

Supporting Reference

1 R. Sun, J. Guo, C. Sun, T. Wang, Z. Luo, Z. Zhang, X. Jiao, W. Tang, C. Yang, Y. Li, J. Min, *Energy Environ. Sci.* 2019, **12**, 384.

2 R. Sun, Q. Wu, J. Guo, T. Wang, Y. Wu, B. Qiu, Z. Luo, W. Yang, Z. Hu, J. Guo, M. Shi, C. Yang, F. Huang, Y. Li, J. Min, *Joule* 2020, **4**, 407.

3 K. Weng, L. Ye, L. Zhu, J. Xu, J. Zhou, X. Feng, G. Lu, S. Tan, F. Liu, Y. Sun, *Nat. Commun.*2020, **11**, 2855.

4 X. Xie, J. Liao, J. Liu, Y. Meng, W. Huang, X. Zhan, L.-M. Wang, Q. Li, T. Zhu, S. Liu, Y.-P. Cai, *Phys. Status Solidi RRL* 2021, **15**, 2100386.

5 K. Jiang, J. Zhang, Z. Peng, F. Lin, S. Wu, Z. Li, Y. Chen, H. Yan, H. Ade, Z. Zhu, A. K. Y. Jen, *Nat. Commun.* 2021, **12**, 468.

6 Y. Zhang, K. Liu, J. Huang, X. Xia, J. Cao, G. Zhao, P. W. K. Fong, Y. Zhu, F. Yan, Y. Yang, X. Lu, G. Li, *Nat. Commun.* 2021, **12**, 4815.

7 L. Zhan, S. Li, X. Xia, Y. Li, X. Lu, L. Zuo, M. Shi, H. Chen, *Adv. Mater.* 2021, **33**, 2007231.

8 J. Chen, J. Cao, L. Liu, L. Xie, H. Zhou, J. Zhang, K. Zhang, M. Xiao, F. Huang, *Adv. Funct. Mater.* 2200629.

9 L. Ye, Y. Cai, C. Li, L. Zhu, J. Xu, K. Weng, K. Zhang, M. Huang, M. Zeng, T. Li, E. Zhou, S. Tan, X. Hao, Y. Yi, F. Liu, Z. Wang, X. Zhan, Y. Sun, *Energy Environ. Sci.* 2020, **13**, 5117.

10 J. Cai, H. Wang, X. Zhang, W. Li, D. Li, Y. Mao, B. Du, M. Chen, Y. Zhuang, D. Liu, H.-L. Qin, Y. Zhao, J. A. Smith, R. C. Kilbride, A. J. Parnell, R. A. L. Jones, D. G. Lidzey, T. Wang, *J. Mater. Chem. A* 2020, **8**, 4230.

11 Y. Zhang, Y. Cho, J. Lee, J. Oh, S.-H. Kang, S. M. Lee, B. Lee, L. Zhong, B. Huang, S. Lee, J.-W. Lee, B. J. Kim, Y. Li, C. Yang, *J. Mater. Chem. A* 2020, **8**, 13049.

12 R. Yu, H. Yao, Y. Xu, J. Li, L. Hong, T. Zhang, Y. Cui, Z. Peng, M. Gao, L. Ye, Z. a. Tan, J. Hou, *Adv. Funct. Mate.r* 2021, **31**, 2010535.

13 H. Fan, H. Yang, Y. Wu, O. Yildiz, X. Zhu, T. Marszalek, P. W. M. Blom, C. Cui, Y. Li, *Adv. Funct. Mater.* 2021, **31**, 2103944.

14 J. Fu, S. Chen, K. Yang, S. Jung, J. Lv, L. Lan, H. Chen, D. Hu, Q. Yang, T. Duan, Z. Kan, C. Yang, K. Sun, S. Lu, Z. Xiao, Y. Li, *iScience* 2020, **23**, 100965.

15 X. Wang, L. Zhang, L. Hu, Z. Xie, H. Mao, L. Tan, Y. Zhang, Y. Chen, *Adv. Funct. Mater.* 2021, **31**, 2102291.

16 R. Yu, G. Wu, Y. Cui, X. Wei, L. Hong, T. Zhang, C. Zou, S. Hu, J. Hou, Z. a. Tan, *Small* 2021, **17**, 2103497